Check for updates

Iron-saturated bovine lactoferrin: a promising chemopreventive agent for hepatocellular carcinoma†

Hury Viridiana Hernández-Galdámez,[a] Samia Fattel-Fazenda,‡[a]
Teresita N. J. Flores-Téllez,[b] Mario Alejandro Aguilar-Chaparro,[a]
Jonathan Mendoza-García,[a] Lidia C. Díaz-Fernández,[a] Eunice Romo-Medina,[a]
Yesennia Sánchez-Pérez,[c] Jaime Arellanes-Robledo, [ID][d] Mireya De la Garza,[a]
Saúl Villa-Treviño*[a] and Carolina Piña-Vázquez [ID] *[a]

Hepatocellular carcinoma (HCC) is a tumor with minimal chance of cure due to underlying liver diseases, late diagnosis, and inefficient treatments. Thus, HCC treatment warrants the development of additional strategies. Lactoferrin (Lf) is a mammalian multifunctional iron-binding glycoprotein of the innate immune response and can be found as either a native low iron form (native-Lf) or a high iron form (holo-Lf). Bovine Lf (bLf), which shares many functions with human Lf (hLf), is safe for humans and has several anticancer activities, including chemotherapy boost in cancer. We found endogenous hLf is downregulated in HCC tumors compared with normal liver, and decreased hLf levels in HCC tumors are associated with shorter survival of HCC patients. However, the chemoprotective effect of 100% iron saturated holo-bLf on experimental hepatocarcinogenesis has not yet been determined. We aimed to evaluate the chemopreventive effects of holo-bLf in different HCC models. Remarkably, a single dose (200 mg kg^{-1}) of holo-bLf was effective in preventing early carcinogenic events in a diethylnitrosamine induced HCC *in vivo* model, such as necrosis, ROS production, and the surge of facultative liver stem cells, and eventually, holo-bLf reduced the number of preneoplastic lesions. For an established HCC model, holo-bLf treatment significantly reduced HepG2 tumor burden in xenotransplanted mice. Finally, holo-bLf in combination with sorafenib, the advanced HCC first-line treatment, synergistically decreased HepG2 viability by arresting cells in the G0/G1 phase of the cell cycle. Our findings provide the first evidence suggesting that holo-bLf has the potential to prevent HCC or to be used in combination with treatments for established HCC.

1. Introduction

Liver cancer is the sixth most common neoplasm and the third most lethal, with more than 780 000 deaths per year

[a]*Departamento de Biología Celular, Centro de Investigación y de Estudios Avanzados del IPN (CINVESTAV-IPN), CDMX, Mexico. E-mail: svilla@cinvestav.mx, carolina.pina@cinvestav.mx*
[b]*Cancer Research UK Manchester Institute, The University of Manchester, Alderley Park, SK10 4TG Macclesfield, UK*
[c]*Instituto Nacional de Cancerología (INCan), Subdirección de Investigación Básica, CDMX, Mexico*
[d]*Laboratorio de Enfermedades Hepáticas, Instituto Nacional de Medicina Genómica, Ciudad de México, México. Dirección de Cátedras, Consejo Nacional de Humanidades, Ciencias y Tecnologías (CONAHCYT), Ciudad de México, Mexico*
†Electronic supplementary information (ESI) available. See DOI: https://doi.org/10.1039/d3fo05184f
‡Deceased.

worldwide.[1] Hepatocellular carcinoma (HCC) accounts for more than 80% of primary liver cancers.[2] Major risk factors for HCC include HBV and HCV infection, diabetes, excess alcohol consumption and metabolic liver disease, particularly nonalcoholic fatty liver disease. Early HCC stage is amenable for potential curative treatment, such as local ablation, surgical resection and liver transplantation; unfortunately, only 20 to 30% of patients are eligible for such interventions since most of them have already reached an advanced cancer stage at the first HCC diagnosis.[3] Of note, despite its side effect profile and poor improvement in overall survival (OS) of less than three months, sorafenib has been the first-line systemic treatment.[4] Consequently, HCC has limited options for curative strategies due to underlying liver diseases, late diagnosis and inefficient treatments.

Thus, as with most human malignancies, HCC progression needs to be challenged using different strategies. Cancer

chemoprevention, defined as the use of pharmacological agents, either natural or synthetic, is a strategy to delay, reverse, suppress or prevent disease pathogenesis, such as cancer.[5] Lactoferrin (Lf) is an 80 kDa iron-binding multifunctional glycoprotein of the innate immune response that is mainly found in milk and other mammalian exocrine secretions. It can be iron free, containing either less than 5% (apo-Lf) or 100% of iron (holo-Lf), the saturated form. Native Lf, which is secreted under physiological conditions, contains 10 to 20% iron saturation; however, in inflammatory or infected microenvironments, holo-Lf prevails because of the high iron concentration.[6]

Bovine lactoferrin (bLf) has been classified as a human Lf (hLf) bioequivalent because of the high sequence homology that shares many functions. It has been involved in several protective activities, such as antioxidant, immunomodulatory, antimicrobial and anticancer activities.[6] Several studies have demonstrated that bLf is tolerated and has no toxicity in humans; moreover, it has been approved by both the USA Food and Drug Administration (FDA) and the European Food Safety Authority (EFSA) as a dietary supplement in food products.[7,8] Interestingly, the chemopreventive effects of bLf have been demonstrated in several animal models bearing different tumor types, including lung, tongue, esophagus, and colorectal cancer, showing that bLf has been effective in inhibiting growth, metastasis, and tumor-associated angiogenesis, as well as potentiating chemotherapy.[6] Clinical trials in patients with colorectal polyps revealed that native-bLf has chemopreventive potential.[9,10] bLf binds specifically to the asialoglycoprotein receptor (ASGPR), which is expressed in the hepatocyte membrane and has been found to be conserved in HCC biopsies.[11] Therefore, it is feasible to propose that HCC might be an attractive target of the antitumoral effects of bLf. For instance, native-bLf has been shown to have chemopreventive effects when it is simultaneously and daily administered either for several weeks or two weeks before a hepatocarcinogenic agent.[12–14]

Most research on the anticancer capabilities of bLf has been performed by using native-bLf, and it has been proposed that iron saturation in Lf is irrelevant for its anticancer effects.[15] In contrast, other studies have demonstrated that iron saturation does affect the anticancer capabilities of bLf. In vitro studies have shown divergent results in breast cancer cell lines. MDA-MB-231 and MCF-7 cells showed more sensitivity to the cytotoxic effects of native-bLf than holo-bLf,[16] or MDA-MB-231, MCF-7, T-47D and Hs578T cells were more sensitive to holo-bLf, followed by native-bLf and apo-bLf.[17] In human glioblastoma cells, holo-bLf was found to be more effective in inducing anti-migratory activity than the native one, both at the cellular and molecular levels.[18] Furthermore, in vivo experiments have shown that holo-bLf is effective in inhibiting tumorigenesis and increasing the chemotherapy capability to eliminate EL-4 lymphoma, while bLf saturated with lower levels of iron failed to synergize with chemotherapy to eradicate tumors.[19] Although the exact mechanism by which holo-bLf surpasses the less saturated bLf form in vivo is

unknown, the above data strongly suggest that holo-bLf has potential as a therapeutic agent.[16]

Based on the anticancer capability of native-bLf, some studies have shown its chemopreventive effects on rodent models of diethylnitrosamine (DEN)-induced hepatocarcinogenesis;[12] however, the chemopreventive effects of holo-bLf on hepatocarcinogenesis have not yet been investigated. Therefore, it is plausible to determine whether the anticancer capability of holo-bLf is more effective than that of native-bLf. The aim of this investigation was to evaluate the chemopreventive effects of holo-bLf on HCC progression at multiple levels by challenging both in vivo and in vitro HCC models. Additionally, the simultaneous effect of holo-bLf and sorafenib on an in vitro HCC model was also investigated. The present study introduces the first exploration of holo-bLF as a chemopreventive agent in HCC, advancing our understanding of bLf anticancer effect, and providing a novel avenue for advanced HCC treatment research.

2. Materials and methods

2.1 Design of this work

Our study is organized in three phases, utilizing both in vivo and in vitro methodologies. In the initial phase, we evaluated the effectiveness of two forms of bLf (native and holo) as chemopreventive agents during the early stages of hepatocarcinogenesis (from 2 to 30 days) using an in vivo model of chemical hepatocarcinogenesis in Fischer-344 rats. bLf was administered as a single dose prior to exposure to the first carcinogen DEN. The analytical assessments included the quantification of necrosis, ROS lipid peroxidation, stem cell markers onset, and preneoplastic lesions. The second phase focused on the effect of holo-bLf on established HCC. First, we used an in vitro model with HCC cell lines (HepG2 and Hep3B) and determined the cell viability after treatment with holo-bLf. Subsequently, a xenotransplantation model with hepG2 cells was used to test the effect of holo-bLf on in vivo tumor growth. The third phase of the study investigated the in vitro combination effect of holo-bLf with sorafenib: first-line treatment vs. advanced HCC treatment. Viability assays were also conducted for that purpose, and alterations in the cell cycle were evaluated. This comprehensive and integrated approach ensures a thorough understanding of the effects of holo-bLf as a chemopreventive agent for HCC at multiple levels: early hepatocarcinogenesis, established HCC and as a combinational approach with first-line therapy for HCC.

2.2 Reagents and antibodies

Bovine lactoferrin (97.01% purity) in the iron-poor form native-bLf, 20% iron-saturated, was purchased from NutriScience (Trumbull, USA). Reagents including DEN (N0756, St Louis, Missouri USA), 2-acetylaminofluorene (2-AAF, A7015, St Louis, Missouri USA), and 2′,7′-dichlorodihydrofluorescein diacetate (DCFH-DA, D6883, St Louis, Missouri, USA) were purchased from Sigma Chemical Co. (St Louis, Missouri,

USA). The AldeRed ALDH Detection Assay kit (01700, Vancouver, British Columbia, Canada) and anti-CD44v6 (AB2080 Temecula, CA, USA) were purchased from Millipore. Antibodies against CD90 (202508, San Diego CA, USA) and CD45 (202205 San Diego, CA, USA) were from BioLegend; anti-CD133 was from GeneTex (GTX12295, San Antonio, TX, USA); and anti-CD24 was from BD Pharmingen (562104, Franklin Lakes, NJ, USA).

2.3 hLf gene (LTF) expression analysis in HCC patient cohorts from public databases

The UCSC Xena browser tool (https://xenabrowser.net/) was used to download hLf gene (LTF) expression in the HCC cohort of The Cancer Genome Atlas (TCGA) based upon data generated by Research Network: https://www.cancer.gov/tcga (TCGA-LIHC) and in the normal liver tissue cohort of The Genotype Tissue Expression (GTEx) database (https://www.gtex-portal.org/home/). The Mann–Whitney test was used to compare both expression levels. The GSE136247[20] and GSE113996 (https://www.ncbi.nlm.nih.gov/geo/query/acc.cgi?acc=GSE113996) cohorts were downloaded from the Gene Expression Omnibus (GEO) at (https://www.ncbi.nlm.nih.gov/geo/) and analyzed using paired t tests. Kaplan–Meier plots were generated for the TCGA-LIHC cohort using KM plot (https://kmplot.com/analysis/index.php?p=background) to calculate the cutoff value and for data download. The log-rank (Mantel–Cox) test was used to compare the differences in survival curves.

2.4 Preparation of iron-binding protein

Holo-bLf was produced by dissolving native-bLf in 40 mM Tris/20 mM sodium bicarbonate buffer (pH 7.4) to have a final protein concentration of 200 μM. It was saturated with iron by adding 400 μM ferric chloride and incubated at 4 °C overnight with agitation. Unbound iron was removed by dialysis using SnakeSkin™ Dialysis Tubing (pore size was 12 000 Da) (Thermo Scientific Cat. 68100, Rockford Illinois, USA), with water as the dialysis buffer, with six changes for 36 h.[21] The protein was concentrated by ultrafiltration in an Amicon® ultra centrifugal filter 30 kDa (Millipore, Cat. UFC903008, Tullagreen, Carrigtwohill, Co Cork Ireland) and stored at −20 °C. Protein concentrations were determined by the Bradford micromethod.[22] The iron concentration was determined by the IRON-TPTZ colorimetric method (Spinreact). Holo-bLf resulted in an Fe saturation ≤90%.

2.5 Animal procedures

All experiments were performed under the Institutional Animal Care and Use Committee Guidelines and according to protocol No. 0168-15, approved by the Committee for the Care and Use of Laboratory Animals (CICUAL) of CINVESTAV-IPN. Animals were obtained from the Unit for Production of Experimental Laboratory Animals (UPEAL CINVESTAV, Mexico City, Mexico). Animals had free access to food, standard diet (PMI Feeds Inc., Laboratory Diet) and water. They were main-

tained in a holding room under controlled conditions of a 12 h light/dark cycle, 50% relative humidity and 21 °C.

2.6 Hepatocarcinogenesis model and bLf administration

A modified version of the resistant hepatocyte protocol for inducing hepatocarcinogenesis was used. Briefly, male Fischer-344 rats weighing ∼200 g were intragastrically administered 200 mg kg^{-1} DEN once, followed by intragastric administration of 20 mg kg^{-1} 2-AAF on days 3, 4, and 5, as previously reported (manuscript in preparation).[8] The bLf was intragastrically administered once 24 h before DEN (Fig. 2A). Rats were euthanized by isoflurane anesthesia and exsanguination, and pieces of liver were frozen in liquid nitrogen for cryopreservation and stored at −75 °C for further analysis. Other pieces were fixed in 4% formalin and embedded in paraffin for histological analysis.

2.7 Necrosis quantification

The liver tissue was treated as previously described by Macias-Perez et al. 2013.[23] The extent of necrosis was quantified in 10 fields/rat at 100X using an Olympus IX70 microscope with the AnalySIS Opty Soft Imaging System GmbH 3.00 (Olympus Europa GmbH, Hamburg, Germany). Necrotic areas were defined as acellular regions adjacent to cells with pale pink cytoplasm, nuclear dissolution (karyolysis), and/or nuclear fragmentation (karyorrhexis), cellular debris and inflammatory infiltrates.[24] Using this definition, the necrotic areas were calculated by quantifying the normal area (not necrotic nor acellular) and subtracting it from the total area in the microscopic field.[23,25]

2.8 Lipid peroxidation determination

Fifty milligrams of frozen liver were processed as previously described.[26] Briefly, tissue was homogenized in 1 ml of a buffer containing 100 mM Tris, 150 mM NaCl and 1 mM Phenylmethylsulfonyl fluoride (PMSF) at pH 7.4. Subsequently, 50 μl of the total homogenate was combined with 30 μl of a solution comprising 150 mM Tris pH 7.4 and 300 μl of 0.4% thiobarbituric acid (TBA) dissolved in 20% acetic acid at pH 3. The mixture was homogenized and was incubated at 100 °C for 1 hour until complete evaporation of the liquid. Following this, the samples were placed on ice for 10 min, and 200 μl of a solution containing 1.2% KCl and 500 μl of pyridine/butanol (1 : 15) was added. Tubes were the centrifugated at 6000g for 15 min at 4 °C. Duplicate transfers of 200 μl of the resulting supernatant were made to a 96-well plate, and absorbance measurements were conducted at a wavelength of 532 nm using a plate reader Thermo Scientific Additionally, a 1 : 10 dilution of the initial homogenate was performed to determine protein concentration using the Bradford method. The results were expressed with respect to malondialdehyde (MDA) by using the MDA extinction coefficient ($E = 1.56 \times 10^5$) as nmol of MDA per mg of total protein.

2.9 ROS quantification

Fifty milligrams of frozen liver were treated as previously described.[27] Breafly, tissue was homogenized in 1 ml of a buffer comprising 100 mM Tris, 150 mM NaCl and 1 mM PMSF at pH 7.4 buffer. Subsequently, 40 μl of the homogenate were added into a 96 well plate, and mixed with 10 μl of 100 μM 2′,7′-dichlorofluorescin diacetate (DCFH-DA) and 50 μl of 150 mM TRIS at pH 7.4. The plate was protected from light and incubated 1 h at room temperature, after that, fluorescence was read at 480 nm excitation/515 nm emission using a TECAN GENious plate reader. Fluorescence was corrected by subtracting blanks in each experiment and autofluorescence of each lysate.

2.10 Flow cytometry analysis

On day six after cancer induction, rats were anesthetized under isoflurane and perfused using a modified two-step collagenase perfusion procedure, and then, liver nonparenchymal cells were separated by centrifugation cycles.[28] Then, isolated cells were incubated at 4 °C for 20 min either with the primary antibodies anti-CD133 (GeneTex Cat. GTX12295), anti-CD44v6 (Millipore Cat. AB2080), anti-CD90 Alexa Fluor® 647 (BioLegend Cat. 202508), anti-CD24 PE (BD Pharmingen Cat. 562104), or anti-CD45 FITC (BioLegend Cat. 202205). Cells incubated with anti-CD133 and anti-CD44v6 were then washed with 2% FBS in PBS and incubated with secondary FITC-labeled anti-rabbit (goat anti-rabbit IgG FITC, Jackson, Cat. 111-095-045, Baltimore Pike, West Grove, PA, USA) for 20 min at 4 °C. Cells were washed once, resuspended in 2% fetal bovine serum (FBS) in PBS and then analyzed. Dead cells were stained either with propidium iodine or blue trypan according to fluorochrome compatibility. To detect aldehyde dehydrogenase-positive cells (ALDH⁺), an AldeRed ALDH detection assay kit was used (Millipore cat. SCR150, Temecula, CA USA) according to the manufacturer's instructions. Cells were analyzed using the BD LSRFortessa™ X-20 cell analyzer, and data were analyzed using BD ModFITT LT v2.0 software.

2.11 γ-Glutamyl transpeptidase (GGT) staining and preneoplastic lesion quantification

Liver preneoplastic lesions were stained to detect the activity of the GGT enzyme, a well-known HCC and altered hepatic foci marker, in 20 μm-thick frozen tissue sections, as previously described.[23,29] Then, GGT-positive (GGT+) foci were captured and quantified using AnalySIS Opty Soft Imaging System GmbH 3.00 software (Olympus Europa GmbH, Hamburg, Germany).

2.12 3-(4,5-Dimethylthiazol-2-yl)-2,5-diphenyltetrazolium bromide (MTT) assay

HepG2 and Hep3B cells were obtained from ATCC, genotyped for authentication and tested for mycoplasma contamination using MycoAlert™ PLUS (Cat. LT07-701, Lonza, Rockland, ME, USA). Cells from passages 20 to 30 were used for the experiments. Cells were maintained in Dulbecco's modified Eagle's medium (DMEM) supplemented with 10% FBS in 5% CO_2 at 37 °C.

Cell viability was determined by MTT assay (Cat. M6494 Invitrogen, Willow Creek Road, CA, USA). Briefly, cells at the exponential growth phase were subcultured and seeded in a 96-well plate (5×10^5 per well). After 48 h of incubation, the culture medium was replaced with fresh medium containing holo-bLF and/or sorafenib (S-8502, LC Laboratories, Woburn, MA, USA). Doses of both holo-bLf and sorafenib were selected based on previous reports.[30–32] For the combination experiments, the sorafenib concentration was 3 or 5 μM, and that of holo-bLf was 50 μM. After 24, 48 or 72 h, cell viability was determined following the manufacturer's protocol. The combination index of sorafenib plus holo-bLf treatment was calculated by CompuSyn software (**https://www.combosyn.com/index.html**), as previously reported.[33]

2.13 Holo-bLf treatment of the xenograft mouse model

HCC xenografts were established in six-week-old female NOD-scid IL2Rγnull (NSG™) mice by the subcutaneous inoculation of 5×10^6 HepG2 cell suspension in 200 μl of 10% FBS in DMEM in the flank region. After two weeks, the tumors reached 0.5 cm^3, and the mice were randomly assigned to two groups ($n = 7$ mice per group). Using a cannula, animals were orally administered vehicle (MQ water) or 200 mg kg^{-1} holo-bLf every other day for 20 days. At the end of the experiment, the mice were euthanized by an anesthesia overdose of ketamine/xylazine; then, the tumors were collected, weighed and stored at −75 °C for further analysis.

2.14 Cell cycle assay

HepG2 cells (1×10^6) were treated with either holo-bLf and/or sorafenib for 24 h, following the protocol described in the previous section. Then, the cells were detached with PBS-EDTA (0.48 mM) and fixed with 70% ethanol at −20 °C for 24 h. After that, the cells were washed twice and processed with a BD Cycletest™ Plus DNA Kit according to the manufacturer's protocol. Samples were read in a BD FACSCanto II cytometer with FACSDiva v.1.1 software. Data were analyzed using BD ModFITT LT v2.0 software.

2.15 Statistical analysis

Data were analyzed using GraphPad Prism software 6.01. All experiments were performed in triplicate. The results are presented as the mean ± standard deviation (SD) or standard error of the mean (SEM). Statistical significance was determined by analysis of variance (ANOVA), Tukey's multiple comparisons test and Student's t test with $p < 0.05$.

3. Results

3.1 hLf gene (LTF) expression is downregulated in HCC tissue

To explore whether Lf has a natural effect on patients HCC progression, we first analyzed the hLf gene (*LTF*) expression
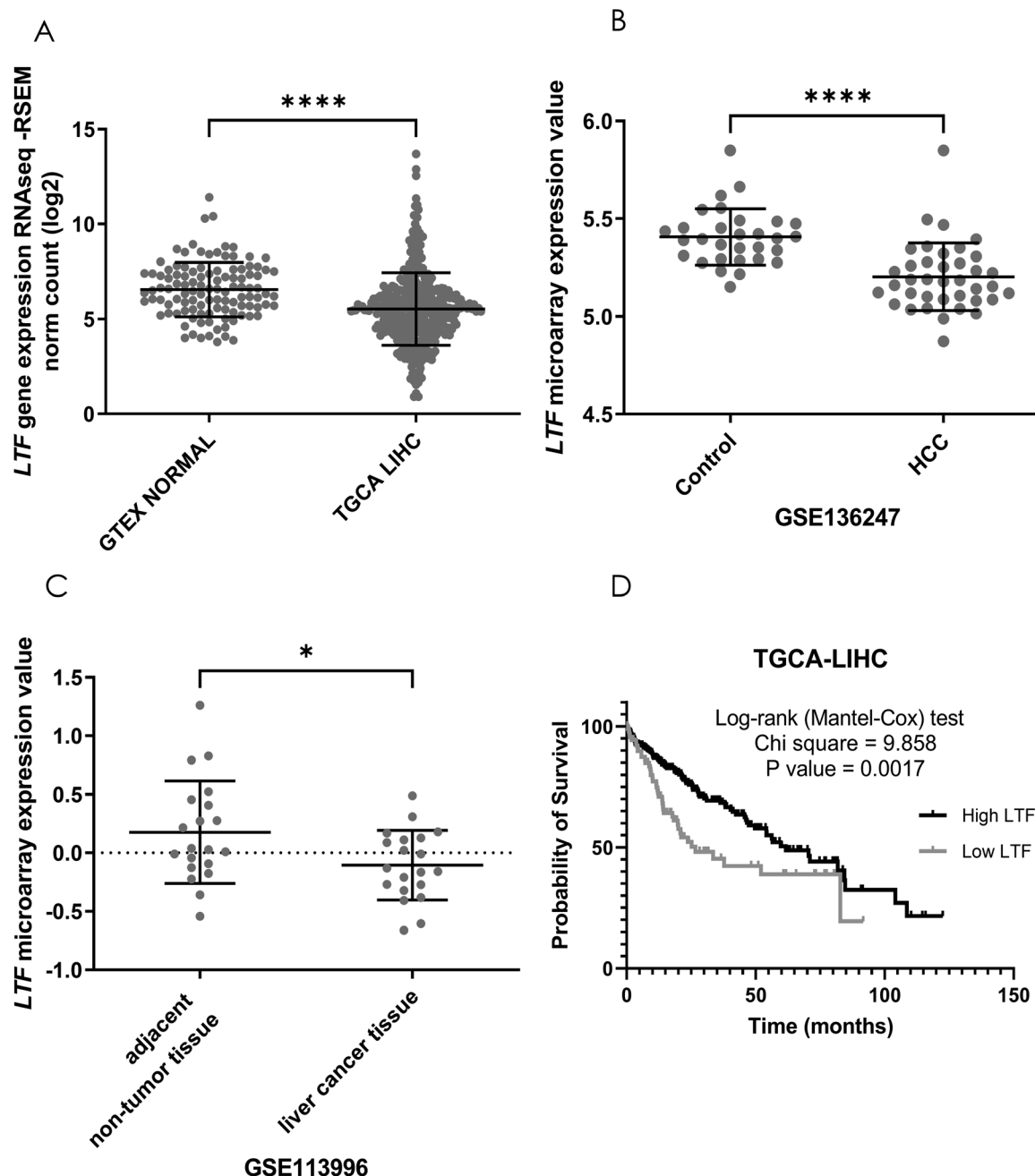
Fig. 1 LTF expression in normal and HCC tissues LTF expression is compared between normal liver tissue and HCC biopsies from the GTEx and TCGA LIHC databases with unpaired t test with Mann-Whitney test (a). LTF expression was compared between HCC-adjacent and tumor tissues from two HCC patient GEO cohorts: GSE136247 (b) and GSE113996 (c) with unpaired t test with Welch's correction. Kaplan–Meier curve of the TCGA LIHC cohort showing overall survival probability in LTF-low patients ($n = 90$) and patients with high expression of LTF ($n = 274$), log-rank (Mantel–Cox) test (d).

profile in HCC patients by comparing *LTF* gene expression in normal liver tissue with HCC biopsies from the Genotype-Tissue Expression (GTEx) database and from The Cancer Genome Atlas database (TCGA-LIHC), respectively. *LTF* expression was significantly ($p < 0.0001$) higher in normal liver than in HCC biopsies (Fig. 1A). We also compared *LTF* gene expression in HCC adjacent tissues *versus* tumor tissue of two GEO cohorts (GSE136247 and GSE113996), confirming that

LTF expression was also higher in adjacent tissue than in tumor samples (Fig. 1B and C). To evaluate the prognostic value of tumoral *LTF* expression in HCC patients, we generated Kaplan–Meier curves of *LTF* gene expression using data from the TCGA-LIHC cohort. We found a difference in the overall survival probability. Samples with lower *LTF* expression exhibited significantly ($p = 0.0017$) shorter survival than those with higher *LTF* expression (Fig. 1D). This evidence suggests that
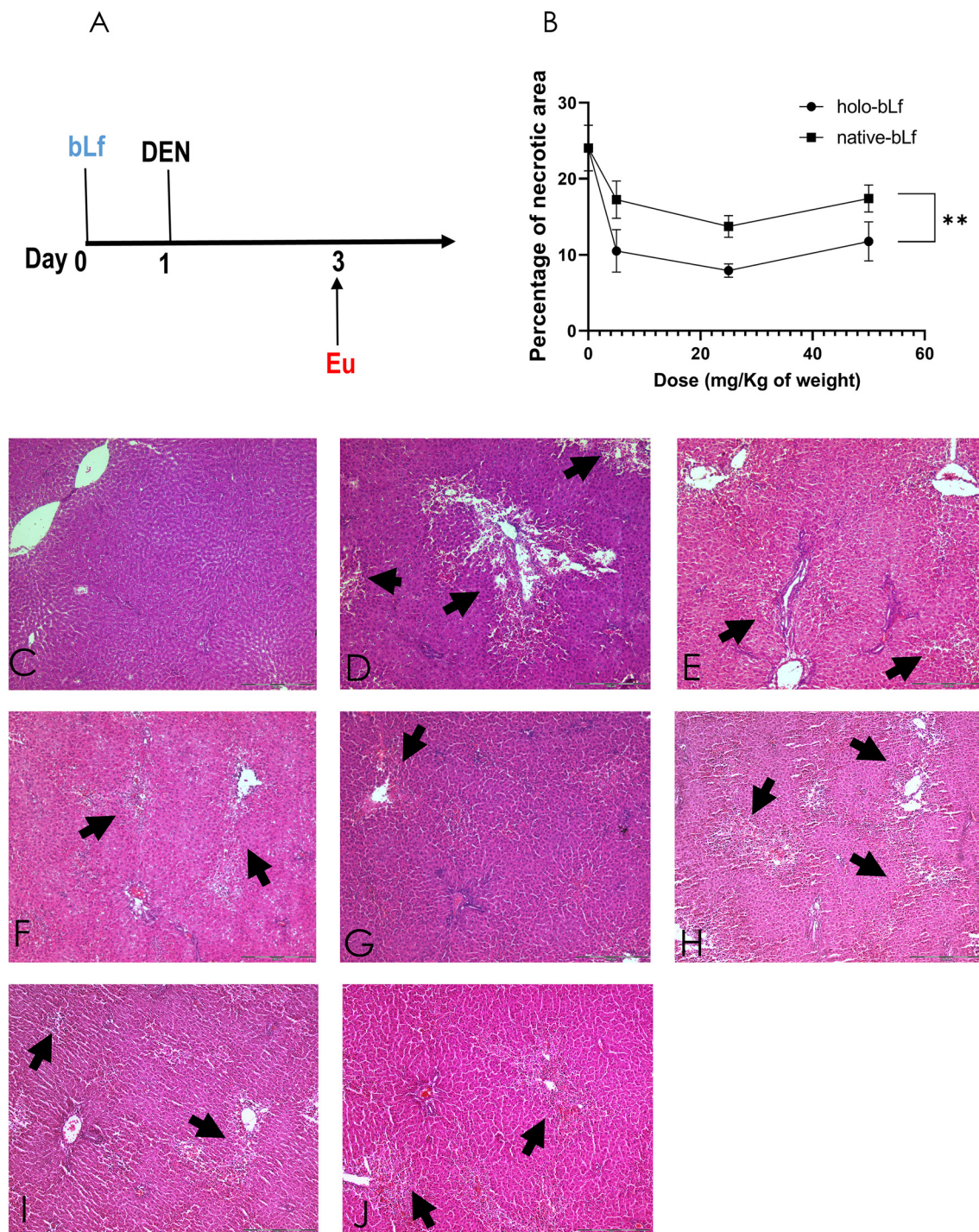
Fig. 2 Effect of bLf on the liver necrotic area induced by DEN. (a) Working scheme, rats were subjected to a single dose of either holo-bLf or native-bLf 24 h before the onset of the carcinogenic treatment. On day 1, DEN was administered, and groups of 4 rats were euthanized (eu) at 48 h after DEN administration. Liver sections were processed with H&E staining, and then, the necrotic area was quantified (b–k). (b) Quantification of the necrotic area. The mean $\pm$ SEM (n = 3) was plotted, and ANOVA and Tukey's multiple comparisons tests were performed. **$p \leq 0.01$. Micrographs of: nontreated group (c). Necrosis observed in the livers of animals subjected to DEN alone was considered 100% damage (d). Groups treated with holo-bLf at (e) 5 mg kg^{-1}, (f) 25 mg kg^{-1}, and (g) 50 mg kg^{-1}. Groups treated with native-bLf at (h) 5 mg kg^{-1}, (i) 25 mg kg^{-1}, and (j) 50 mg kg^{-1}.

endogenous Lf has a protective effect against HCC progression. Furthermore, it has been reported that bLf is a bioequivalent of hLf,[6] and the consumption of bLf increases the hLf serum concentration in patients.[10] Thus, it is not unreasonable to determine the potential of bLf as a chemopreventive agent in HCC *in vivo* models.
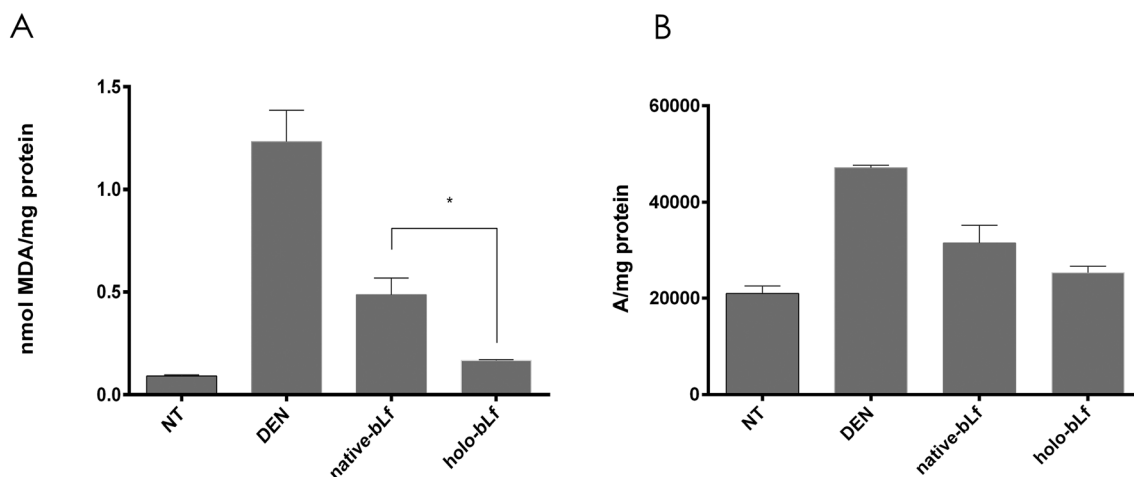
A

B

Fig. 3 Effect of bLf on DEN-induced ROS and lipid peroxidation to determine the effect of holo-bLf and native-bLf on lipid peroxidation, rats were euthanized 48 h after DEN administration. Lipid peroxidation levels are expressed in nmol of mda per mg of protein (a). ROS levels are expressed in arbitrary units per mg of protein (b). The mean $\pm$ SEM (n = 3) was plotted, and ANOVA and Sidak's multiple comparisons tests were performed. *$p \leq$ 0.05.

3.2 Holo-bLf is more efficient than native-bLf in preventing DEN-induced damage and ROS production during the early stages of rat hepatocarcinogenesis

Then, we determined the effectiveness of the two forms of bLf, namely, holo-bLf and native-bLf, to prevent the early hepatocarcinogenesis stages. For this purpose, we used a modified experimental model of hepatocarcinogenesis,[34,35] as shown in Fig. 4A. After a single dose of either holo-bLf or native-bLf was administered to animals before cancer initiation with DEN (Fig. 2A), two variables were evaluated. The first is liver cell necrosis, a phenomenon that plays a key role in promoting early changes associated with liver carcinogenesis induced by DEN.[36] Thus, necrosis was evaluated 48 h after DEN administration either with or without pretreatment with a single dose of holo-bLf or native-bLf (Fig. 2B–J). Holo-bLf was able to significantly (p = 0.0086) prevent DEN-produced necrosis better than native-bLf (Fig. 2B). The dose of 25 mg kg^{-1} was selected for further experiments.

Since DEN metabolism increases reactive oxygen species (ROS) production and elevated oxidative stress correlates with increased malignancy,[37,38] we determined oxidative stress by measuring two parameters, namely, lipid peroxidation and ROS production, 48 h after DEN administration either with or without pretreatment with holo-bLf or native-bLf (Fig. 3). The effect of bLf on lipid peroxidation was evaluated by measuring malondialdehyde (MDA), the main metabolite of lipid peroxidation.[26] Holo-bLf pretreatment significantly (p = 0.0294) reduced lipid peroxidation more than native-bLf (Fig. 3A). ROS measurement showed no significant difference between holo-bLf and native-bLf pretreatments; however, there was a tendency for holo-bLf pretreatment to perform moderately better in reducing ROS levels (Fig. 3B). This result showed that pretreatment with a single dose of holo-bLf was more efficient than that of native-bLf in preventing DEN-induced necrosis

and ROS production. Based on this evidence, we decided to use only holo-bLf hereinafter.

3.3 Holo-bLf decreases the surge in stem cell markers during hepatocarcinogenesis

Carcinogenic schemes based on DEN and 2-acetylaminofluorene (2AAF) are proposed to rely on their capability to induce local tissue damage and proliferative repair that expand the cell population susceptible to undergo malignant transformation.[39] Such populations are nonparenchymal cells known as facultative liver stem or progenitor cells (LSPCs), which drive liver compensatory regeneration.[39] Importantly, inhibition of LSPC proliferation in chronically injured mouse livers significantly reduces HCC development in several models.[40–42] Therefore, we determined the effect of holo-bLf on some of the cells that emerge after carcinogenic induction using well-known stem cell markers, such as CD133, ALDH, CD90, CD24, and CD44v6.[43] One day after the last carcinogenic insult (Fig. 4A), positive cells increased, but pretreatment with bLf prevented this phenomenon by reducing the percentage of ALDH$^+$-, CD133-, and CD24-positive cells to normal levels, except for CD90, which diminished significantly more than the control (p = 0.001133) (Fig. 4B).

3.4 A single dose of holo-bLf before cancer initiation prevents the appearance of preneoplastic lesions

To determine whether holo-bLf has the capability to prevent the appearance of preneoplastic lesions, we administered a single oral dose of holo-bLf before liver cancer initiation. Rats then received the carcinogenic treatment and were sacrificed 30 days after initiation (Fig. 4C). GGT histochemistry analysis was performed to detect preneoplastic lesions in liver tissue (Fig. 4D–F). The results showed a significant (p = 0.0444) reduction in the number of preneoplastic lesions (Fig. 4G). A
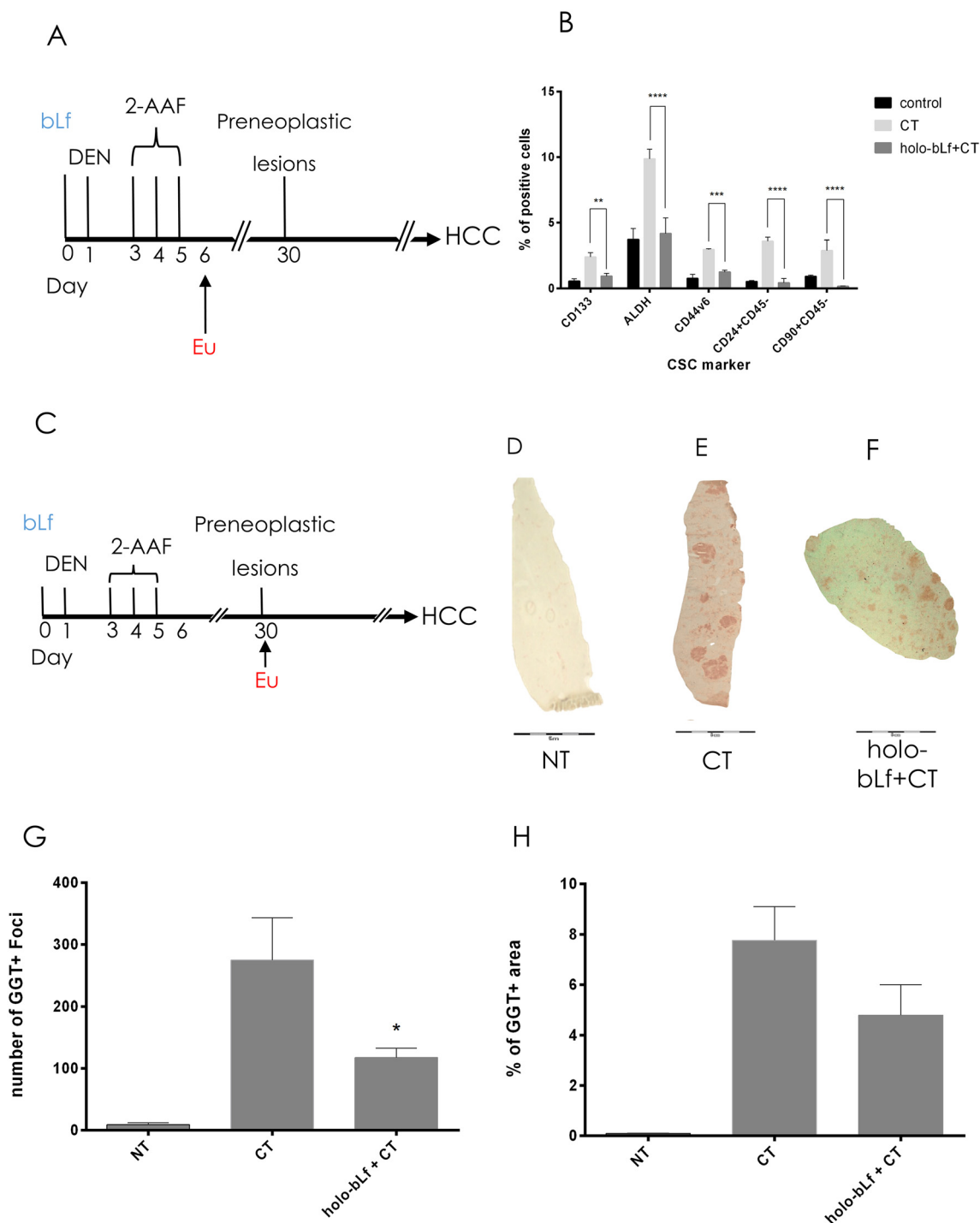
Fig. 4 Effect of pretreatment with a single dose of holo-bLf on the surge in stem cells and preneoplastic lesion appearance. (a) Working scheme, rats were given a single dose of holo-bLf 24 h before cancer initiation. Animals were euthanized (eu) 1 day after the last 2-AAF dose. (b) Plots represent nonparenchymal cells positive for CD133, CD44v6, CD24, CD45, CD90 and ALDH$^+$. The percentage of positive cells was determined by flow cytometry. Mean $\pm$ SD was plotted, ANOVA and Tukey's multiple comparisons tests were performed (n = 3), and significances were calculated as compared with carcinogenic treatment (CT) are shown: *$p \leq 0.05$, **$p \leq 0.01$, ***$p \leq 0.001$, ****$p \leq 0.0001$. (c) Working scheme, rats were subjected to a single dose of holo-bLf 24 h before cancer initiation. Animals rats were euthanized (eu) 30 days after the last 2-AAF dose. Liver frozen sections were stained to detect preneoplastic lesions by GGT activity. (d) Untreated animals (NT); (e) animals subjected to complete carcinogenic treatment (CT); (f) animals subjected to holo-bLf treatment before cancer initiation. (g) Number of GGT-positive foci. (h) Percentage of GGT-positive area. The mean $\pm$ SEM was plotted, unpaired student's t test was performed, and significant differences were calculated compared with the CT group: *$p \leq 0.05$. n = 3 per group.
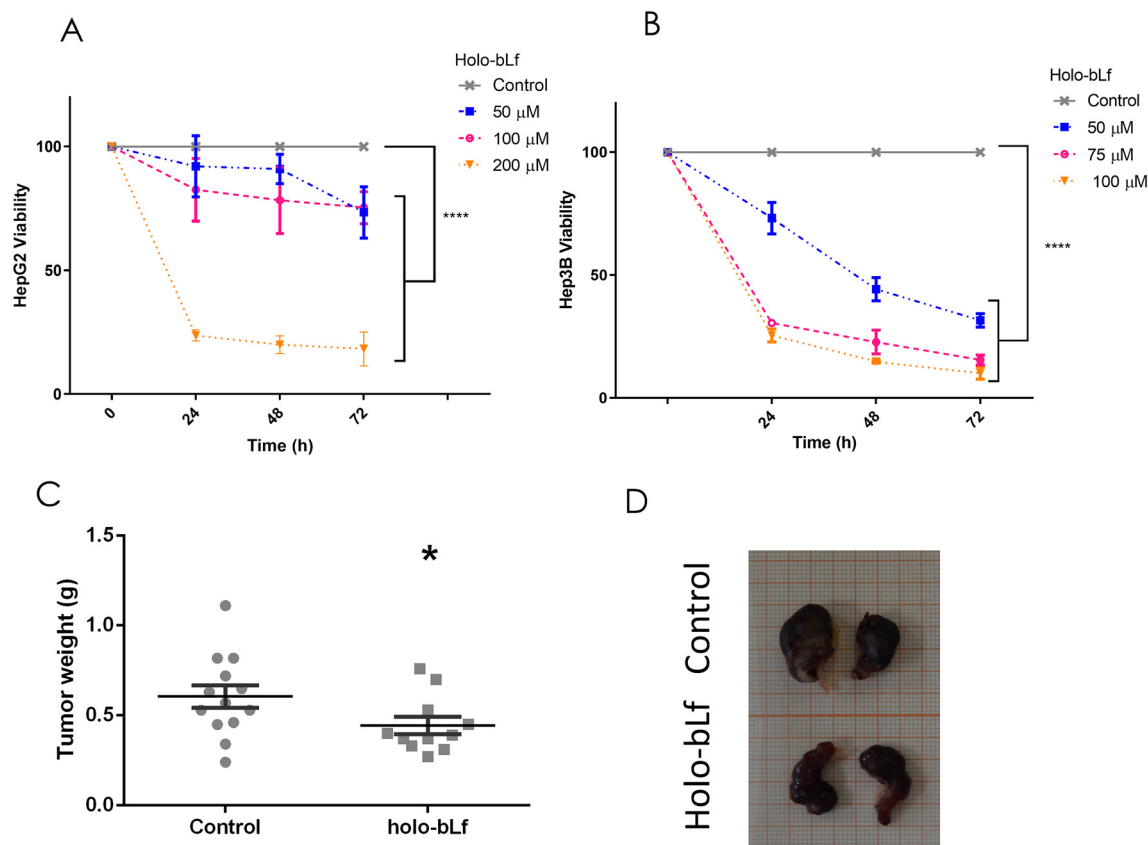
Fig. 5 Effect of holo-bLf on xenografted HCC tumors. HepG2 or Hep3B cells were incubated with different concentrations of either holo-bLf for the indicated times, followed by an MTT assay. Viability plots are shown (a) HepG2 or (b) Hep3B cells were treated with holo-bLf at 50, 100 and 200 μm or 50, 75 and 100 μm, respectively, for 24, 48, 72 and 96 h ($n = 9$), two-way ANOVA Tukey's multiple comparisons test. Xenografted tumors were established for 15 days in the flanks of NSG mice using HepG2 cells. Then, the oral administration of either vehicle ($n = 7$) or holo-bLf (200 mg kg^{-1}, $n = 6$) every other day for 20 days was performed. (c) Plot of tumor weight at the end of the experiment (day 35). Plot showing the mean ± SEM. Significant differences were calculated by unpaired student's t test and compared with the untreated group. *$p \leq 0.05$. (d) Representative images showing excised tumors.

no significant tendency toward a reduction in the percentage of preneoplastic area was observed (Fig. 4H). This result suggests that holo-bLf has a chemopreventive effect on early HCC stages.

3.5 Holo-bLf reduces tumor burden in a xenograft mouse model

To determine the effect of holo-bLf on an established HCC tumor, its effect on two HCC cell lines, HepG2 and Hep3B, was evaluated. Holo-bLf was able to decrease the viability of HepG2 cells by 68% during the first 24 h and by 82% after 72 h of treatment with the higher dose of 200 μM (Fig. 5A), while Hep3B viability was decreased by 75% within 24 h and up to 90% after 72 h with the higher dose of 100 μM (Fig. 5B). Next, we xenotransplanted 5×10^6 HepG2 cells in NSG immunodeficient mice. Fifteen days later, when tumors reached 0.5 cm^3, holo-bLf was orally administered every other day for 20 days. 200 mg kg^{-1} dose of holo-bLf was chosen based on Li et al. report (Li, Li et al. 2017).[67] Mice were sacrificed, and tumor weights were recorded (Fig. 5C and D). The results

showed that holo-bLf alone was able to reduce the tumor burden in xenotransplanted mice by 26.7% compared with the vehicle group ($p = 0.0301$) (Fig. 5C). This result proposes that holo-bLf has the ability to decrease established HCC tumors.

3.6 Holo-bLf and sorafenib synergistically inhibit the viability of HepG2 cells in vitro

Lactoferrin has been used in combination with several chemotherapeutics and has been shown to improve their antitumoral effects in different cancers,[44,45] while sorafenib is the first-line treatment for advanced HCC, despite its modest increase in OS and considerable side effects.[4] Here, we aimed to test the effect of different doses of sorafenib and holo-bLf and to determine either their synergistic or additive effect using their lowest antitumoral doses on the viability of HepG2 and Hep3B cells. The combination of a sublethal dose of holo-bLf (Fig. 5A) and sorafenib (Fig. 6A), namely, 50 μM and 3 μM, respectively,[46] decreased HepG2 cell viability by 33% at 24 h, 91.4% at 48 h and 98.8% at 72 h. The combination index (CI)
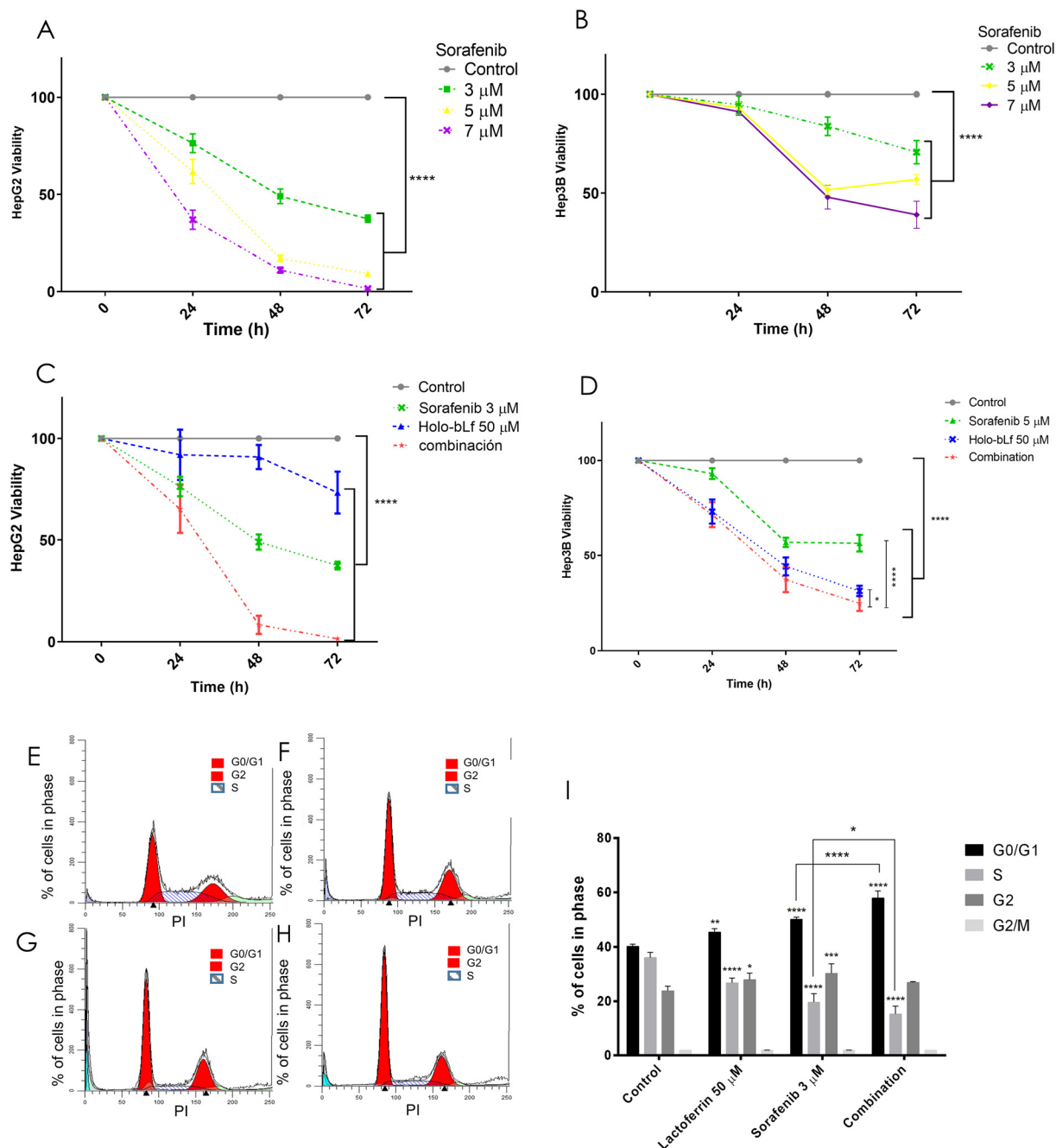
Fig. 6 Synergistic cytotoxic effect of holo-bLf and sorafenib on the arrest of HepG2 cells in G0/G1 phase of the cell cycle. HepG2 or Hep3B cells were incubated with different concentrations of either holo-bLf and/or sorafenib for the indicated times, followed by an MTT assay. Viability plots are shown. (a) HepG2 ($n = 6$) or (b) Hep3B cells ($n = 9$) were treated with sorafenib at 3, 5 and 7 µm for 24, 48 and 72 h. (c) HepG2 ($n = 6$) or (d) Hep3B cells ($n = 9$) were treated with 3 or 5 µm sorafenib, respectively, in combination with 50 µm holo-bLf for 24, 48 and 72. For cell cycle analysis, HepG2 cells were treated with 50 µm holo-bLf and/or 3 or 5 µm sorafenib for 24 h, and then the cells were fixed and stained as described in the materials and methods. Cells were analyzed by flow cytometry. (e–h) Representative histograms of the DNA content of (e) control cells treated with (f) holo-bLf, (g) sorafenib, and (h) the combination. (i) Percentage of cells in each cell cycle phase. Data represent the mean $\pm$ SD, $n = 3$. ANOVA and Tukey's multiple comparisons tests were performed, and significant differences were calculated compared with either the control group or specific comparisons. $*p < 0.05$, $**p < 0.005$, $****p < 0.0001$.

for 48 and 72 h was 0.54 and 0.41, respectively (Fig. 6C). This evidence showed that a synergistic interaction between both compounds induced a cytotoxic effect that decreased the viability of HepG2 cells.[47] The Hep3B cells exhibited a comparable

trend, demonstrating a statistically significant difference between the combined effect and the individual compound effects, albeit without reaching additive or synergistic interactions (Fig. 6B and D).

3.7 Holo-bLf in combination with sorafenib induces the arrest of HepG2 cells in G0/G1 phase of the cell cycle

bLf has been previously shown to induce cell cycle arrest in different cancer cell types.[6] To investigate a possible mechanism involved in the decrease in cell viability induced by the synergistic effect of holo-bLf and sorafenib, we investigated whether the cell cycle was affected. HepG2 cells were incubated with holo-bLf and/or sorafenib for 24 h, and then the cells were analyzed by flow cytometry to determine cell cycle progression. HepG2 cells treated with holo-bLf showed a higher percentage of cells in G0/G1 (113% ± 0.82) and a lower percentage of cells in S phase (74% ± 1.80) when compared with controls. Sorafenib treatment increased the percentage of cells in G0/G1 (124.87% ± 0.78) and decreased that in S phase (54.42% ± 3.20), alongside an increase in G2 phase (126.93% ± 3.50) when compared with controls. The combination of both compounds increased the number of cells in G0/G1 by 143.99% ± 2.63, while the number of cells in S phase decreased to 42.41% ± 2.85 when compared with controls (Fig. 6E–H). This result clearly shows that both holo-bLf and sorafenib induce the arrest of HepG2 cells in the G0/G1 phase of the cell cycle when they are separately administered. Importantly, the combined administration induced a stronger increase in cell arrest in G0/G1 phase (Fig. 6I). Thus, these results provide evidence supporting the synergistic action of holo-bLf and sorafenib in reducing the viability of HepG2 cells, indicating that holo-bLf contributes to cell cycle arrest, thereby enhancing the cytotoxicity beyond that achieved by sorafenib alone.

4. Discussion and conclusions

We performed an *in silico* analysis of tumor samples from three HCC patient cohorts, showing that the human *LTF* gene is downregulated in tumor tissue compared to healthy individual liver samples or adjacent tissue. This finding is consistent with the fact that Lf is highly expressed in noncancerous cell lines compared to cancer cell lines.[48] We also found that TCGA-LIHC HCC patients with higher *LFT* expression had significantly better survival than those with low LFT expression, which strongly suggests that hLf might protect against liver cancer in humans. It has been reported that bLf is bioequivalent to hLf;[6] moreover, bLf consumption increases the hLf serum concentration in patients.[10] This evidence, along with our *in silico*, *in vivo* and *in vitro* findings, points to a prospective chemopreventive role of bLf in humans and as a potential compound for combinational therapy for HCC patients.

bLf has been previously proven to be a chemopreventive agent in experimental HCC models; however, for the first time, we evaluated the chemopreventive effectiveness of a different iron-saturated form of bLf on HCC progression. The capability of holo-bLf and native-bLf to lessen the early alterations induced by the carcinogen DEN was evaluated, showing that holo-bLf was more effective than native-bLf in reducing DEN-induced necrosis. A plausible explanation for this phenomenon is its greater digestive stability, resulting in higher bio-

availability of holo-bLf than that of either native-bLf or apo-bLf.[49] Another possibility is that the molecular conformation caused by iron binding might result in differential receptor recognition and possibly in the activation of different signaling pathways downstream, such as that of the immune response.[18] Further research is needed to validate these proposals.

Resistant hepatocyte models have been used for decades for the study of HCC progression.[34] This model uses DEN, a well-known hepatocarcinogen, and one of the byproducts of DEN metabolism is reactive oxygen species (ROS), which cause a procarcinogenic increase in oxidative stress.[38] Additionally, it has been proposed that necrosis induced by DEN plays a key role in the early stages of experimental hepatocarcinogenesis, probably by stimulating compensatory cell proliferation.[36] Cell proliferation is required for the induction of resistant hepatocytes (referred to as initiated hepatocytes resistant to the mitostatic 2AAF effect) during initiation by carcinogens such as DEN.[36] DEN is a procarcinogen that needs to be activated by cytochrome P450 isoforms, such as CYP1A1/2, CYP2B1/2, and CYP2E1, in the rat liver.[50,51] Native bLf has the ability to reduce MeIQx-induced CYP1A2 levels,[12] 7,12-dimethylbenz[*a*]anthracene (DMBA)-induced CYP1A1 levels,[52] and able to suppress alcohol-induced liver injury-induced overexpression of cytochrome P450 2E1 (CYP2E1).[53] Therefore, based on the temporality of holo-bLf exposure in this study, it is not unreasonable to propose that holo-bLf might inhibit cytochrome P450 isoforms that activate DEN metabolism and, as a result, reduce DEN activation. Previous studies suggest that reducing hepatocyte cell death and compensatory proliferation, as long as oxidative stress has a pronounced beneficial effect, protects against carcinogenesis.[54] Thus, holo-bLf might work as a chemopreventive agent that blocks DEN activation, inhibiting cancer initiation, granting this would need experimental confirmation.

Another mechanism might be associated with the antioxidant role of bLf. During carcinogenesis, ROS might activate protumorigenic signaling, enhance cell survival and proliferation, and drive DNA damage and genetic instability.[55] We have previously reported a close correlation between the induction of ROS-derived liver lipoperoxidation and the appearance of preneoplastic lesions.[38] On the other hand, the antioxidant potential of bLf has been widely documented;[52,56,57] however, it has been mostly attributed to the iron sequestering capability of native- or apo-bLf, since iron is a well-known prooxidant that induces ROS production through the Fenton reaction.[58] Therefore, we verified that iron-saturated bLf did not increase ROS production beyond the increase produced by DEN. Notably, we found that holo-bLf decreased ROS production and has a tendency to reduce lipid peroxidation beyond the effect induced by native-bLf. Thus, iron content does not appear to affect the antioxidant effect of bLf in our experimental model. Supporting this evidence, it has been reported that bLF has ROS-scavenging capability and protects DNA from direct oxidative damage *in vitro*, independently of its iron saturation degree.[59] In a hamster buccal pouch carcinogenesis model, native-bLF increases its antioxidant capa-

bility by elevating the GSH/GSSG ratio and GPx activity in the liver.[60] Such antioxidant mechanisms could be unrelated to Lf iron content and therefore contribute to the antioxidant activity of holo-bLf observed in our model, an intriguing phenomenon that needs further confirmation.

In our *in vivo* model, holo-bLf reduced the number of pre-neoplastic lesions but did not modify their total area, the hypothesis is that holo-bLf pretreatment was able to reduce the number of initiated hepatocytes but did not significantly affect their proliferation. This phenomenon might be due to the unique dose of holo-bLf that animals received 24 h before DEN administration, which was only able to block cancer initiation, but by the time that subsequent alterations appeared, such as increased proliferation of initiated cells, the active form of holo-bLf was either decreased or absent. Further studies using repeated doses of holo-bLf during and after cancer initiation might reveal the potential of holo-bLf to block the proliferation of initiated cells and, as a consequence, reduce the total area of preneoplastic lesions. This hypothesis is supported by the evidence that holo-bLf was able to reduce the proliferation of established HCC both *in vitro* and *in vivo*. Additionally, the effect of holo-bLf on initiated cells could be explained based on the HCC model used. The original model of the resistant hepatocyte relies on the proliferative stimuli given by a partial hepatectomy after the promoter carcinogen 2AAF.[34,35] The model used in this study is a modified version, where 2AAF is administered 48 h after DEN. Closing the time frame between DEN and 2AAF apparently replaces the need for an extra proliferative stimulus, since such stimulus is most likely given exclusively by DEN-associated necrosis.[36] Thus, it is plausible to propose that by reducing DEN-associated necrosis, holo-bLf was able to lessen liver-initiated cells.

This above proposal is also supported by the evidence that bLf diminished the emergence of a subpopulation of liver stem cells early in the carcinogenesis process. The role of cancer stem cells in established cancers has been extensively documented, but their presence during the early carcinogenesis stages has barely been investigated. Rats subjected to severe liver damage and a blockade of hepatocyte proliferation, such as those subjected to the resistant hepatocyte model, present short-lived and highly proliferating cells expressing both cholangiocyte- and hepatocyte-specific markers, as well as the embryonic liver marker AFP.[61] This phenomenon is called a ductular reaction, and the cells are named oval cells. Recently, by lineage tracing experiments in mice, it was confirmed that such cells are derived from biliary epithelial cells and act as facultative liver stem/progenitor cells (LSPCs), which promote compensatory proliferation.[62,63] LSPCs constitute a cell subpopulation susceptible to malignant transformation, and it has been demonstrated that they give rise to HCC tumors.[39,64] However, how early these cells have a definitive commitment toward malignant transformation has not yet been clarified, with the earliest time reported being 5 months.[64] In our investigation, we analyzed the LSPC subpopulation very early, *i.e.*, one day postcarcinogenic treatment, using a wide panel of CSC markers and discovered that holo-bLf was able to significantly reduce LSPCs by identifying CD133 and one CD44 isoform (CD44v6). Although we did not investigate their commitment degree toward malignant transformation at the early carcinogenesis stage, it is probable that some of those LSPCs have already started their transformation since all carcinogenic insults have already acted, to eventually, namely, several months, progress toward HCC. The relevance of this subpopulation during carcinogenesis has been evidenced by some recent studies showing that by diminishing the LSPC surge, carcinogenesis might be prevented.[41,42,65]

Our investigation represents the first report showing that Lf inhibits established HCC tumors *in vivo*. The dose of bLf chosen was within the low range of *in vivo* doses used by other authors;[19,66] specifically, a 200 mg kg^{-1} dose of holo-bLf was chosen based on the findings of Li *et al.*[67] Previous studies have reported that bLf doses up to 4 g kg^{-1} are safe by demonstrating no to cause any toxicological lesions in male F344 rat organs.[68] In fact, for infants aged 0–6 months, bLf intake is set by the EFSA at 200 mg per kg body weight and 1.2 g day^{-1}.[69] Of note, in our investigation, the tumors were reduced by 26.7%; similarly, a previous report showed that holo-bLf diminished the tumor burden by 37% in a mouse model of 4T1 breast cancer cells.[44] Immunomodulation is considered to play a major role in Lf tumor suppression activity, mainly through stimulation of NK cells and CD4+ and CD8+ T cells.[6] We used an extremely immunodeficient mouse strain named NOD-scid IL2Rγnull (NSG™), which lacks mature T cells, B cells, and NK cells; they are "nonleaky" and produce defective DCs.[70] Therefore, our results also demonstrate an immune independence of T cells, B cells, and NK cells for holo-bLf *in vivo* antitumoral activity against HCC cells.

Sorafenib is the first-line treatment for advanced HCC patients, despite its modest impact on survival and toxicity. Because of its adverse effects, it has been necessary to combine sorafenib with other drugs to lower its dose and to improve tolerability without losing effectiveness[4] To determine whether the combination of holo-bLf and sorafenib has an additive or synergistic effect on HCC cell viability, we determined the combination index (CI) using the software CompuSyn (https://www.combosyn.com). This calculation is based on the Chou–Talalay theory used to assess the statistical significance of combination experiments,[71] and this method is currently accepted for calculating synergy and additivity.[47,72] CI < 1 indicates synergism, CI = 1 indicates an additive effect, and CI > 1 indicates antagonism. The combination indices we obtained for HepG2 cells were CI = 0.54 after 48 h and CI = 0.41 after 72 h (Fig. 6C); therefore, we concluded that the effect of the combination of holo-bLf and sorafenib on *in vitro* HepG2 cell viability was synergistic. Such a combined effect on Hep3B cells was moderated with the tested doses, although significantly different from holo-bLf or sorafenib alone. Sorafenib is a multikinase inhibitor, and one of its targets is the Ras-Raf-MAPK axis; however, it has been reported that its inhibitory activity prompts the compensatory activation of PI3K-Akt-mTOR signaling. On the other hand, bLf decreases the phosphorylation of Akt and mTOR in several models.[17,73]

Therefore, we can hypothesize that the combination of holo-bLf and sorafenib acts synergistically because they simultaneously inhibit the Ras-Raf-MAPK and PI3K-Akt-mTOR axes.

Here, we also found that holo-bLf and sorafenib either individually or in combination induced G0/G1 cell cycle arrest. The effect of holo-bLf on the arrest of cancer cell lines in G0/G1 phase is in line with its effect shown in other cancers.[74,75] Sorafenib is reported to cause cell cycle arrest in several cancer cell lines, including HepG2; coincidentally, our investigation showed that it arrested the cell cycle in G0/G1 phase.[76,77]

In conclusion, to our knowledge, this is the first investigation reporting the chemopreventive effect of holo-bLf on HCC. The results suggest that Holo-bLf outperforms native-bLf as a chemopreventive agent in the early stage of an *in vivo* HCC model. Holo-bLf moderately diminishes the tumor burden in established HCC models, whereas *in vitro*, it has a synergic effect when used in combination with sorafenib. Therefore, our investigation suggests that holo-bLf is a promising molecule to prevent HCC and to challenge advanced HCC in combination with sorafenib. Finally, our investigation encourages deeper mechanistic studies of the chemopreventive action of holo-bLf on HCC progression.

Author contributions

Villa-Treviño, Saúl and Piña-Vázquez, Carolina: Conceptualization, funding acquisition; supervision, formal analysis, writing – review & editing. Sánchez-Pérez Yesennia: Resources and supervision. Hernández-Galdámez, Hury Viridiana: Investigation; methodology, visualization, formal analysis, writing – original draft. Fattel-Fazenda, Samia, Aguilar-Chaparro Mario Alejandro, Mendoza-García Jonathan, Díaz-Fernández, Lidia, Romo-Medina Eunice: Methodology. Flores-Téllez, Teresita N. J.: Software, formal analysis, review & editing. De la Garza, Mireya: Conceptualization and resources. Arellanes-Robledo, Jaime: Writing – review & editing.

Abbreviations

HCC	Hepatocellular carcinoma
Lf	Lactoferrin
holo-Lf	Iron saturated Lf
DEN	Diethylnitrosamine
ROS	Reactive oxygen species
ALDH	Aldehyde dehydrogenase
TCGA	The cancer genome atlas
HBV	Hepatitis B virus
HCV	Hepatitis C virus
OS	Overall survival
bLf	Bovine Lf
hLf	Human Lf
FDA	USA food and drug administration
ASGPR	Asialoglycoprotein receptor
2-AAF	2-Acetylaminofluorene
DCFH-DA	2′,7′-Dichlorodihydrofluorescein diacetate
PMSF	Phenylmethylsulfonyl fluoride
TBA	Thiobarbituric acid
MDA	Malonyldialdehyde
AHF	Altered hepatic foci
GGT	γ-Glutamyl transpeptidase
FBS	Fetal bovine serum
PBS	Phosphate buffered saline
HBSS	Hanks' balanced salt solution
LTF	hLf gene
GTEx	The genotype tissue expression
MTT	3-(4,5-dimethylthiazol-2-yl)-2,5-diphenyltetrazolium bromide
DMEM	Dulbecco's Modified Eagle's medium
SD	Standard deviation
SEM	Standard error of the mean
ANOVA	Analysis of variance
LSPCs	Liver stem or progenitor cells
CT	Carcinogenic treatment
DMBA	7,12-Dimethylbenz[*a*]anthracene
GSH	Reduced glutathione
GSSG	Oxidized glutathione
AFP	Alpha fetoprotein

Conflicts of interest

There are no conflicts of interest to declare.

Acknowledgements

References

1 J. Ferlay, M. Laversanne, M. Colombet, L. Mery, M. Piñeros, I. A. Znaor and F. Bray, *Global Cancer Observatory: Cancer Today*, Lyon, France: International Agency for Research on Cancer, **https://gco.iarc.fr/today**, (accessed April 3, 2020).

2 H. B. El-Serag and K. L. Rudolph, Hepatocellular carcinoma: epidemiology and molecular carcinogenesis, *Gastroenterology*, 2007, **132**, 2557–2576.

3 J. D. Yang, P. Hainaut, G. J. Gores, A. Amadou, A. Plymoth and L. R. Roberts, A global view of hepatocellular carcinoma: trends, risk, prevention and management, *Nat. Rev. Gastroenterol. Hepatol.*, 2019, **16**, 589–604.

4 C. Akateh, S. M. Black, L. Conteh, E. D. Miller, A. Noonan, E. Elliott, T. M. Pawlik, A. Tsung and J. M. Cloyd, Neoadjuvant and adjuvant treatment strategies for hepatocellular carcinoma, *World J. Gastroenterol.*, 2019, **25**, 3704–3721.

5 L. K. Penny and H. M. Wallace, The challenges for cancer chemoprevention, *Chem. Soc. Rev.*, 2015, **44**, 8836–8847.

6 A. Cutone, L. Rosa, G. Ianiro, M. S. Lepanto, M. C. Bonaccorsi di Patti, P. Valenti and G. Musci, Lactoferrin's Anti-Cancer Properties: Safety, Selectivity, and Wide Range of Action, *Biomolecules*, 2020, **10**(3), 456.

7 EFSA, Panel on Dietetic Products, Nutrition and Allergies (NDA) Scientific Opinion on bovine lactoferrin, *EFSA J.*, 2012, 2811.

8 A. M. Rulis, Agency Response Letter GRAS Notice No. GRN 000077.

9 M. Iigo, D. B. Alexander, J. Xu, M. Futakuchi, M. Suzui, T. Kozu, T. Akasu, D. Saito, T. Kakizoe, K. Yamauchi, F. Abe, M. Takase, K. Sekine and H. Tsuda, Inhibition of intestinal polyp growth by oral ingestion of bovine lactoferrin and immune cells in the large intestine, *BioMetals*, 2014, **27**, 1017–1029.

10 T. Kozu, G. Iinuma, Y. Ohashi, Y. Saito, T. Akasu, D. Saito, D. B. Alexander, M. Iigo, T. Kakizoe and H. Tsuda, Effect of orally administered bovine lactoferrin on the growth of adenomatous colorectal polyps in a randomized, placebo-controlled clinical trial, *Cancer Prev. Res.*, 2009, **2**, 975–983.

11 D. Trere, L. Fiume, L. B. De Giorgi, G. Di Stefano, M. Migaldi and M. Derenzini, The asialoglycoprotein receptor in human hepatocellular carcinomas: its expression on proliferating cells, *Br. J. Cancer*, 1999, **81**, 404–408.

12 K. Fujita, T. Ohnishi, K. Sekine, M. Iigo and H. Tsuda, Down-regulation of 2-amino-3,8-dimethylimidazo[4,5-f]quinoxaline (MeIQx)-induced CYP1A2 expression is associated with bovine lactoferrin inhibition of MeIQx-induced liver and colon carcinogenesis in rats, *Jpn. J. Cancer Res.*, 2002, **93**, 616–625.

13 R. R. Hegazy, D. F. Mansour, A. A. Salama, R. F. Abdel-Rahman and A. M. Hassan, Regulation of PKB/Akt-pathway in the chemopreventive effect of lactoferrin against diethylnitrosamine-induced hepatocarcinogenesis in rats, *Pharmacol. Rep.*, 2019, **71**, 879–891.

14 M. M. Mohammed, G. Ramadan, M. K. Zoheiry and N. M. El-Beih, Antihepatocarcinogenic activity of whey protein concentrate and lactoferrin in diethylnitrosamine-treated male albino mice, *Environ. Toxicol.*, 2019, **34**, 1025–1033.

15 J. S. Wolf, G. Li, A. Varadhachary, K. Petrak, M. Schneyer, D. Li, J. Ongkasuwan, X. Zhang, R. J. Taylor, S. E. Strome and B. W. O'Malley Jr., Oral lactoferrin results in T cell-dependent tumor inhibition of head and neck squamous cell carcinoma in vivo, *Clin. Cancer Res.*, 2007, **13**, 1601–1610.

16 J. A. Gibbons, J. R. Kanwar and R. K. Kanwar, Iron-free and iron-saturated bovine lactoferrin inhibit survivin expression and differentially modulate apoptosis in breast cancer, *BMC Cancer*, 2015, **15**, 425.

17 Y. Zhang, A. Nicolau, C. F. Lima and L. R. Rodrigues, Bovine lactoferrin induces cell cycle arrest and inhibits mTOR signaling in breast cancer cells, *Nutr. Cancer*, 2014, **66**, 1371–1385.

18 A. Cutone, B. Colella, A. Pagliaro, L. Rosa, M. S. Lepanto, M. C. Bonaccorsi di Patti, P. Valenti, S. Di Bartolomeo and G. Musci, Native and iron-saturated bovine lactoferrin differently hinder migration in a model of human glioblastoma by reverting epithelial-to-mesenchymal transition-like process and inhibiting interleukin-6/STAT3 axis, *Cell. Signalling*, 2020, **65**, 109461.

19 J. R. Kanwar, K. P. Palmano, X. Sun, R. K. Kanwar, R. Gupta, N. Haggarty, A. Rowan, S. Ram and G. W. Krissansen, 'Iron-saturated' lactoferrin is a potent natural adjuvant for augmenting cancer chemotherapy, *Immunol. Cell Biol.*, 2008, **86**, 277–288.

20 J. P. Cerapio, A. Marchio, L. Cano, I. Lopez, J. J. Fournie, B. Regnault, S. Casavilca-Zambrano, E. Ruiz, A. Dejean, S. Bertani and P. Pineau, Global DNA hypermethylation pattern and unique gene expression signature in liver cancer from patients with Indigenous American ancestry, *Oncotarget*, 2021, **12**, 475–492.

21 R. Xiao and W. S. Kisaalita, Iron acquisition from transferrin and lactoferrin by Pseudomonas aeruginosa pyoverdin, *Microbiology*, 1997, **143**(Pt 7), 2509–2515.

22 M. M. Bradford, A rapid and sensitive method for the quantitation of microgram quantities of protein utilizing the principle of protein-dye binding, *Anal. Biochem.*, 1976, **72**, 248–254.

23 J. R. Macias-Perez, O. Beltran-Ramirez, V. R. Vasquez-Garzon, M. E. Salcido-Neyoy, P. A. Martinez-Soriano, M. B. Ruiz-Sanchez, E. Angeles and S. Villa-Trevino, The effect of caffeic acid phenethyl ester analogues in a modified resistant hepatocyte model, *Anti-Cancer Drugs*, 2013, **24**, 394–405.

24 S. A. Elmore, D. Dixon, J. R. Hailey, T. Harada, R. A. Herbert, R. R. Maronpot, T. Nolte, J. E. Rehg, S. Rittinghausen, T. J. Rosol, H. Satoh, J. D. Vidal, C. L. Willard-Mack and D. M. Creasy, Recommendations from the INHAND Apoptosis/Necrosis Working Group, *Toxicol. Pathol.*, 2016, **44**, 173–188.

25 G. Revilla, N. Al Qtaish, P. Caruana, M. Sainz-Ramos, T. Lopez-Mendez, F. Rodriguez, V. Paez-Espinosa, C. Li, N. F. Vallverdu, M. Edwards, A. Moral, J. I. Perez, J. C. Escola-Gil, J. L. Pedraz, I. Gallego, R. Corcoy, M. V. Cespedes, G. Puras and E. Mato, Lenvatinib-Loaded Poly(lactic-co-glycolic acid) Nanoparticles with Epidermal Growth Factor Receptor Antibody Conjugation as a Preclinical Approach to Therapeutically Improve Thyroid Cancer with Aggressive Behavior, *Biomolecules*, 2023, **13**(11), 1647.

26 J. A. Buege and S. D. Aust, Microsomal lipid peroxidation, *Methods Enzymol.*, 1978, **52**, 302–310.

27 R. Cathcart, E. Schwiers and B. N. Ames, Detection of picomole levels of hydroperoxides using a fluorescent dichlorofluorescein assay, *Anal. Biochem.*, 1983, **134**, 111–116.

28 L. Riccalton-Banks, R. Bhandari, J. Fry and K. M. Shakesheff, A simple method for the simultaneous isolation of stellate cells and hepatocytes from rat liver tissue, *Mol. Cell. Biochem.*, 2003, **248**, 97–102.

29 A. M. Rutenburg, H. Kim, J. W. Fischbein, J. S. Hanker, H. L. Wasserkrug and A. M. Seligman, Histochemical and ultrastructural demonstration of gamma-glutamyl transpeptidase activity, *J. Histochem. Cytochem.*, 1969, **17**, 517–526.

30 Y. G. Chung, E. Tak, S. Hwang, J. Y. Lee, J. Y. Kim, Y. Y. Kim, G. W. Song, K. J. Lee and N. Kim, Synergistic effect of metformin on sorafenib in in vitro study using hepatocellular carcinoma cell lines, *Ann. Hepatobiliary Pancreat. Surg.*, 2018, **22**, 179–184.

31 R. Jiang and B. Lonnerdal, Bovine lactoferrin and lactoferricin exert antitumor activities on human colorectal cancer cells (HT-29) by activating various signaling pathways, *Biochem. Cell Biol.*, 2017, **95**, 99–109.

32 J. C. Wei, F. D. Meng, K. Qu, Z. X. Wang, Q. F. Wu, L. Q. Zhang, Q. Pang and C. Liu, Sorafenib inhibits proliferation and invasion of human hepatocellular carcinoma cells via up-regulation of p53 and suppressing FoxM1, *Acta Pharmacol. Sin.*, 2015, **36**, 241–251.

33 N. Zhang, J. N. Fu and T. C. Chou, Synergistic combination of microtubule targeting anticancer fludelone with cytoprotective panaxytriol derived from panax ginseng against MX-1 cells in vitro: experimental design and data analysis using the combination index method, *Am. J. Cancer Res.*, 2016, **6**, 97–104.

34 D. Solt and E. Farber, New principle for the analysis of chemical carcinogenesis, *Nature*, 1976, **263**, 701–703.

35 E. Semple-Roberts, M. A. Hayes, D. Armstrong, R. A. Becker, W. J. Racz and E. Farber, Alternative methods of selecting rat hepatocellular nodules resistant to 2-acetylaminofluorene, *Int. J. Cancer*, 1987, **40**, 643–645.

36 T. S. Ying, D. S. Sarma and E. Farber, Role of acute hepatic necrosis in the induction of early steps in liver carcinogenesis by diethylnitrosamine, *Cancer Res.*, 1981, **41**, 2096–2102.

37 M. R. McLoughlin, D. J. Orlicky, J. R. Prigge, P. Krishna, E. A. Talago, I. R. Cavigli, S. Eriksson, C. G. Miller, J. A. Kundert, V. I. Sayin, R. A. Sabol, J. Heinemann, L. O. Brandenberger, S. V. Iverson, B. Bothner, T. Papagiannakopoulos, C. T. Shearn, E. S. J. Arner and E. E. Schmidt, TrxR1, Gsr, and oxidative stress determine hepatocellular carcinoma malignancy, *Proc. Natl. Acad. Sci. U. S. A.*, 2019, **116**, 11408–11417.

38 Y. Sanchez-Perez, C. Carrasco-Legleu, C. Garcia-Cuellar, J. Perez-Carreon, S. Hernandez-Garcia, M. Salcido-Neyoy, L. Aleman-Lazarini and S. Villa-Trevino, Oxidative stress in carcinogenesis. Correlation between lipid peroxidation and induction of preneoplastic lesions in rat hepatocarcinogenesis, *Cancer Lett.*, 2005, **217**, 25–32.

39 L. Zhu, D. Finkelstein, C. Gao, L. Shi, Y. Wang, D. Lopez-Terrada, K. Wang, S. Utley, S. Pounds, G. Neale, D. Ellison, A. Onar-Thomas and R. J. Gilbertson, Multi-organ Mapping of Cancer Risk, *Cell*, 2016, **166**, 1132–1146.

40 R. A. Davies, B. Knight, Y. W. Tian, G. C. Yeoh and J. K. Olynyk, Hepatic oval cell response to the choline-deficient, ethionine supplemented model of murine liver injury is attenuated by the administration of a cyclo-oxygenase 2 inhibitor, *Carcinogenesis*, 2006, **27**, 1607–1616.

41 B. Knight, J. E. Tirnitz-Parker and J. K. Olynyk, C-kit inhibition by imatinib mesylate attenuates progenitor cell expansion and inhibits liver tumor formation in mice, *Gastroenterology*, 2008, **135**, 969–979.

42 K. P. Lee, J. H. Lee, T. S. Kim, T. H. Kim, H. D. Park, J. S. Byun, M. C. Kim, W. I. Jeong, D. F. Calvisi, J. M. Kim and D. S. Lim, The Hippo-Salvador pathway restrains hepatic oval cell proliferation, liver size, and liver tumorigenesis, *Proc. Natl. Acad. Sci. U. S. A.*, 2010, **107**, 8248–8253.

43 T. N. Flores-Tellez, S. Villa-Trevino and C. Pina-Vazquez, Road to stemness in hepatocellular carcinoma, *World J. Gastroenterol.*, 2017, **23**, 6750–6776.

44 X. Sun, R. Jiang, A. Przepiorski, S. Reddy, K. P. Palmano and G. W. Krissansen, "Iron-saturated" bovine lactoferrin improves the chemotherapeutic effects of tamoxifen in the treatment of basal-like breast cancer in mice, *BMC Cancer*, 2012, **12**, 591.

45 A. Varadhachary, J. S. Wolf, K. Petrak, B. W. O'Malley Jr., M. Spadaro, C. Curcio, G. Forni and F. Pericle, Oral lactoferrin inhibits growth of established tumors and potentiates conventional chemotherapy, *Int. J. Cancer*, 2004, **111**, 398–403.

46 T. Morisaki, M. Umebayashi, A. Kiyota, N. Koya, H. Tanaka, H. Onishi and M. Katano, Combining celecoxib with sorafenib synergistically inhibits hepatocellular carcinoma cells in vitro, *Anticancer Res.*, 2013, **33**, 1387–1395.

47 K. R. Roell, D. M. Reif and A. A. Motsinger-Reif, An Introduction to Terminology and Methodology of Chemical Synergy-Perspectives from Across Disciplines, *Front. Pharmacol.*, 2017, **8**, 158.

48 E. Hoedt, S. Hardiville, C. Mariller, E. Elass, J. P. Perraudin and A. Pierce, Discrimination and evaluation of lactoferrin and delta-lactoferrin gene expression levels in cancer cells and under inflammatory stimuli using TaqMan real-time PCR, *BioMetals*, 2010, **23**, 441–452.

49 F. J. Troost, J. Steijns, W. H. Saris and R. J. Brummer, Gastric digestion of bovine lactoferrin in vivo in adults, *J. Nutr.*, 2001, **131**, 2101–2104.

50 J. J. Espinosa-Aguirre, J. Rubio, I. Lopez, R. Nosti and J. Asteinza, Characterization of the CYP isozyme profile induced by cyclohexanol, *Mutagenesis*, 1997, **12**, 159–162.

51 L. Verna, J. Whysner and G. M. Williams, N-nitrosodiethylamine mechanistic data and risk assessment: bioactivation, DNA-adduct formation, mutagenicity, and tumor initiation, *Pharmacol. Ther.*, 1996, **71**, 57–81.

52 P. V. Letchoumy, K. V. Mohan, J. J. Stegeman, H. V. Gelboin, Y. Hara and S. Nagini, In vitro antioxidative potential of lactoferrin and black tea polyphenols and protective effects in vivo on carcinogen activation, DNA damage, proliferation, invasion, and angiogenesis during experimental oral carcinogenesis, *Oncol. Res.*, 2008, **17**, 193–203.

53 D. Li, Q. He, H. Yang, Y. Du, K. Yu, J. Yang, X. Tong, Y. Guo, J. Xu and L. Qin, Daily Dose of Bovine Lactoferrin Prevents Ethanol-Induced Liver Injury and Death in Male Mice by Regulating Hepatic Alcohol Metabolism and Modulating Gut Microbiota, *Mol. Nutr. Food Res.*, 2021, **65**, e2100253.

54 A. Wree, C. D. Johnson, J. Font-Burgada, A. Eguchi, D. Povero, M. Karin and A. E. Feldstein, Hepatocyte-specific Bid depletion reduces tumor development by suppressing inflammation-related compensatory proliferation, *Cell Death Differ.*, 2015, **22**, 1985–1994.

55 J. N. Moloney and T. G. Cotter, ROS signalling in the biology of cancer, *Semin. Cell Dev. Biol.*, 2018, **80**, 50–64.

56 N. A. Abdel Baky, A. H. Al-Najjar, H. A. Elariny, A. S. Sallam and A. A. Mohammed, Pramipexole and Lactoferrin ameliorate Cyclophosphamide-Induced haemorrhagic cystitis via targeting Sphk1/S1P/MAPK, TLR-4/NF-kappaB, and NLRP3/caspase-1/IL-1beta signalling pathways and modulating the Nrf2/HO-1 pathway, *Int. Immunopharmacol.*, 2022, **112**, 109282.

57 O. S. Mohamed, N. A. Abdel Baky, M. M. Sayed-Ahmed and A. H. Al-Najjar, Lactoferrin alleviates cyclophosphamide induced-nephropathy through suppressing the orchestration between Wnt4/beta-catenin and ERK1/2/NF-kappaB signaling and modulating klotho and Nrf2/HO-1 pathway, *Life Sci.*, 2023, **319**, 121528.

58 H. Shoji, S. Oguchi, K. Shinohara, T. Shimizu and Y. Yamashiro, Effects of iron-unsaturated human lactoferrin on hydrogen peroxide-induced oxidative damage in intestinal epithelial cells, *Pediatr. Res.*, 2007, **61**, 89–92.

59 Y. Ogasawara, M. Imase, H. Oda, H. Wakabayashi and K. Ishii, Lactoferrin directly scavenges hydroxyl radicals and undergoes oxidative self-degradation: a possible role in protection against oxidative DNA damage, *Int. J. Mol. Sci.*, 2014, **15**, 1003–1013.

60 K. V. Chandra Mohan, R. Kumaraguruparan, D. Prathiba and S. Nagini, Modulation of xenobiotic-metabolizing enzymes and redox status during chemoprevention of hamster buccal carcinogenesis by bovine lactoferrin, *Nutrition*, 2006, **22**, 940–946.

61 C. J. Hindley, G. Mastrogiovanni and M. Huch, The plastic liver: differentiated cells, stem cells, every cell?, *J. Clin. Invest.*, 2014, **124**, 5099–5102.

62 J. O. Russell, W. Y. Lu, H. Okabe, M. Abrams, M. Oertel, M. Poddar, S. Singh, S. J. Forbes and S. P. Monga, Hepatocyte-Specific beta-Catenin Deletion During Severe Liver Injury Provokes Cholangiocytes to Differentiate Into Hepatocytes, *Hepatology*, 2019, **69**, 742–759.

63 A. Raven, W. Y. Lu, T. Y. Man, S. Ferreira-Gonzalez, E. O'Duibhir, B. J. Dwyer, J. P. Thomson, R. R. Meehan, R. Bogorad, V. Koteliansky, Y. Kotelevtsev, C. Ffrench-Constant, L. Boulter and S. J. Forbes, Cholangiocytes act as facultative liver stem cells during impaired hepatocyte regeneration, *Nature*, 2017, **547**, 350–354.

64 G. He, D. Dhar, H. Nakagawa, J. Font-Burgada, H. Ogata, Y. Jiang, S. Shalapour, E. Seki, S. E. Yost, K. Jepsen, K. A. Frazer, O. Harismendy, M. Hatziapostolou, D. Iliopoulos, A. Suetsugu, R. M. Hoffman, R. Tateishi, K. Koike and M. Karin, Identification of liver cancer progenitors whose malignant progression depends on autocrine IL-6 signaling, *Cell*, 2013, **155**, 384–396.

65 Y. W. Zheng, T. Tsuchida, T. Shimao, B. Li, T. Takebe, R. R. Zhang, Y. Sakurai, Y. Ueno, K. Sekine, N. Ishibashi, M. Imajima, T. Tanaka and H. Taniguchi, The CD133+ CD44+ precancerous subpopulation of oval cells is a therapeutic target for hepatocellular carcinoma, *Stem Cells Dev.*, 2014, **23**, 2237–2249.

66 Y. Aoyama, A. Naiki-Ito, K. Xiaochen, M. Komura, H. Kato, Y. Nagayasu, S. Inaguma, H. Tsuda, M. Tomita, Y. Matsuo, S. Takiguchi and S. Takahashi, Lactoferrin Prevents Hepatic Injury and Fibrosis via the Inhibition of NF-kappaB Signaling in a Rat Non-Alcoholic Steatohepatitis Model, *Nutrients*, 2021, **14**(1), 42.

67 H. Y. Li, M. Li, C. C. Luo, J. Q. Wang and N. Zheng, Lactoferrin Exerts Antitumor Effects by Inhibiting Angiogenesis in a HT29 Human Colon Tumor Model, *J. Agric. Food Chem.*, 2017, **65**, 10464–10472.

68 S. Tamano, K. Sekine, M. Takase, K. Yamauchi, M. Iigo and H. Tsuda, Lack of chronic oral toxicity of chemopreventive bovine lactoferrin in F344/DuCrj rats, *Asian Pac. J. Cancer Prev.*, 2008, **9**, 313–316.

69 N. EFSA, Panel on Dietetic Products and Allergies, Scientific Opinion on bovine lactoferrin, *EFSA J.*, 2012, **10**, 2701.

70 L. D. Shultz, B. L. Lyons, L. M. Burzenski, B. Gott, X. Chen, S. Chaleff, M. Kotb, S. D. Gillies, M. King, J. Mangada, D. L. Greiner and R. Handgretinger, Human lymphoid and myeloid cell development in NOD/LtSz-scid IL2R gamma null mice engrafted with mobilized human hemopoietic stem cells, *J. Immunol.*, 2005, **174**, 6477–6489.

71 T. C. Chou, Drug combination studies and their synergy quantification using the Chou-Talalay method, *Cancer Res.*, 2010, **70**, 440–446.

72 D. Duarte and N. Vale, Evaluation of synergism in drug combinations and reference models for future orientations in oncology, *Curr. Res. Pharmacol. Drug Discov.*, 2022, **3**, 100110.

73 X. X. Xu, H. R. Jiang, H. B. Li, T. N. Zhang, Q. Zhou and N. Liu, Apoptosis of stomach cancer cell SGC-7901 and regulation of Akt signaling way induced by bovine lactoferrin, *J. Dairy Sci.*, 2010, **93**, 2344–2350.

74 E. Damiens, I. El Yazidi, J. Mazurier, I. Duthille, G. Spik and Y. Boilly-Marer, Lactoferrin inhibits G1 cyclin-depen-

dent kinases during growth arrest of human breast carcinoma cells, *J. Cell. Biochem.*, 1999, **74**, 486–498.

75 Y. Xiao, C. L. Monitto, K. M. Minhas and D. Sidransky, Lactoferrin down-regulates G1 cyclin-dependent kinases during growth arrest of head and neck cancer cells, *Clin. Cancer Res.*, 2004, **10**, 8683–8686.

76 A. A. Bahman, M. S. I. Abaza, S. I. Khoushiash and R. J. Al-Attiyah, Sequencedependent effect of sorafenib in combi-

nation with natural phenolic compounds on hepatic cancer cells and the possible mechanism of action, *Int. J. Mol. Med.*, 2018, **42**, 1695–1715.

77 B. Yurdacan, U. Egeli, G. Guney Eskiler, I. E. Eryilmaz, G. Cecener and B. Tunca, Investigation of new treatment option for hepatocellular carcinoma: a combination of sorafenib with usnic acid, *J. Pharm. Pharmacol.*, 2019, **71**, 1119–1132.